Influence of Moisture on Broadband Dielectric Properties of the Impregnated Transformer Paper Insulation

Mr. Cheng Jialu[1] and Mr. Hans Edin[2]

Affiliation: [1]Megger Hong Kong; Email:jialu.cheng@megger.com
[2] Royal Institute of Technology, Sweden; Email: edin.hans@kth.se

ABSTRACT

The actual life of a transformer is determined by ageing of the cellulose insulation such as Kraft paper. The presence of moisture in the insulation system decreases the electrical strength of paper and accelerates the aging. An efficient way to monitor the moisture content in paper insulation is to measure the dielectric frequency response of the paper. The moisture dependent permittivity of impregnated transformer paper below 1 MHz has been widely investigated. The frequency response of the paper between 1 kHz and 1 MHz doesn't show significant differences with different moisture contents. Higher frequency dielectric spectroscopy (>1 MHz) is needed to understand the influence of moisture better. The higher frequency range up to GHz is investigated by the Transmission/Reflection technique. Paper insulation is placed in a coaxial line and the scattering parameters are obtained by the modern Vector Network Analyzer. Full wave analysis is utilized to calculate the permittivity from the obtained S-parameters due to its high accuracy. It is proved that moisture in paper makes the response curves shift towards higher frequencies over a wide frequency range. Due to the dimension limitation of the standard coaxial line, the starting frequency is 100 MHz instead of 1 MHz.

Index Terms—Transformer, insulation, Kraft paper, dielectric frequency response, coaxial line, scattering parameter, Transmission/Reflection, permittivity, Vector Network Analyzer, discontinuous

1.0 INTRODUCTION

Power transformer coils are typically insulated with impregnated Kraft paper and immersed in mineral oil. Paper made with cellulose fibers is preferred as insulation material due to its low cost and good overall electrical and mechanical properties. Paper can absorb considerable amount of moisture which decreases both electrical and mechanical strength. Therefore, when a transformer is manufactured, transformer insulation has to be dried in the oven to make the moisture content as low as possible.

The destructive effects of water include: expansion of paper insulation, altering the mechanic pressure of the transformer clamping system; loss of insulation ability and accelerating thermal aging.

Power transformers need to be carefully monitored throughout their operation. Transformer owners need to assess the state of the paper insulation for planning maintenance or renewal. The prevailing method to evaluate the moisture inside insulation is to measure the dielectric frequency response of the transformer in the field by IDAX [1]. After the measurement, data is compared with the data base obtained from the lab experiment to estimate the moisture inside pressboard/paper.

Low frequency dielectric spectroscopy has been widely investigated by many researchers. The variation of the spectroscopy with different moisture contents below 1 kHz is quite remarkable. Above that, there is only slight difference between the frequency response curves with different moisture contents. One measured response of some kind of Kraft paper Termo 70 in [2] shows that it is quite hard to tell the permittivity difference if the frequency is above 1 kHz.

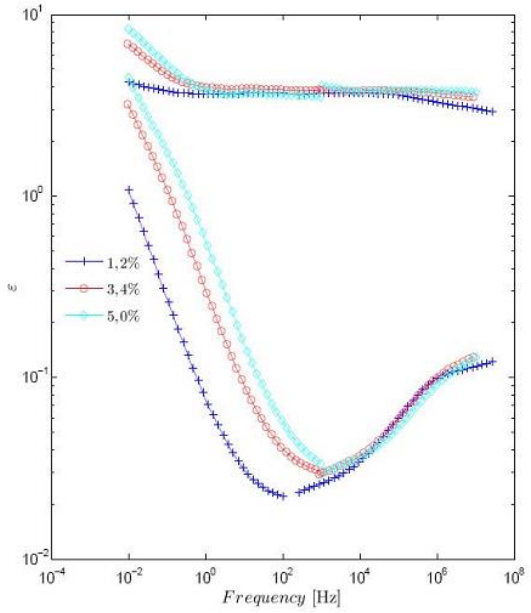

Fig. 1: Master curve for Termo 70 at varying moisture contents. Upper curves represent the real part of the complex permittivity and lower curves represent the imaginary part.

This paper aims to study the influence of moisture on Kraft paper over a wide frequency range from 10 mHz to a few GHz. The instruments involved in the dielectric response measurement are IDAX 300, HP/Agilent 4284A precision LCR meter and the Vector Network Analyzer VNA Master MS2026B.

2.0 COMPLEX PERMITTIVITY

In electromagnetism, permittivity is a measure of to which extent an electric field polarizes dielectric medium. The response of normal materials to external fields generally depends on the frequency of the field. This frequency dependence reflects the fact that a material's polarization does not respond instantaneously to an applied field. The response must always be causal (arising after the applied field) which can be represented by a phase difference, when the E-filed is stationary sinusoidal. For this reason permittivity is often treated as a complex function:

$$\varepsilon_r^*(j\omega) = \varepsilon_r'(\omega) - j\varepsilon_r''(\omega) \quad (1)$$

where ε_r' is the real part of the permittivity, which is related to the stored energy within the medium. ε_r'' is the imaginary part of the permittivity, which is related to the dissipation (or loss) of energy within the medium.

The conductivity also contributes to the permittivity so if $\varepsilon_{r,p}''$ is the loss caused by polarization:

$$\varepsilon_r'' = \varepsilon_{r,p}'' + \frac{\sigma}{\omega\varepsilon_0} \quad (2)$$

where σ is DC conductivity and ω is the angular frequency. Equation (2) indicates that the conductivity contributes to the low frequency dielectric response to a large extent. As the frequency increases, the polarization loss becomes dominant.

2.2 COMPLEX CAPACITOR MODEL

A set-up called Kelvin guard-ring capacitor [3] was devised in which a parallel plate capacitor was arranged as the key component for the permittivity measurement. The test cell is made of two circular Teflon dishes with 50 mm (*D*) stainless steel electrodes. One of the electrodes has a spring system to provide certain pressure to the sample. The test cell is then connected to IDAX 300 and the LCR meter respectively to obtain the dielectric spectroscopy from 10 mHz to 1MHz.

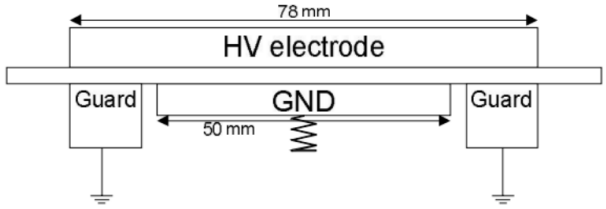

Fig. 2: Schematic diagram of the custom designed Kelvin guard-ring capacitor

The dielectric sample with the thickness of *d* placed between the parallel plates at a particular frequency can be considered electrically equivalent to a capacitor, C_x, in series with a resistor R_x. The values of C_x and R_x are related to the dielectric properties of the sample as:

$$\varepsilon_r' = \frac{C_x}{C_0} \quad (3)$$

$$\tan\delta = \omega C_x R_x = \frac{\varepsilon_r''}{\varepsilon_r'} \quad (4)$$

where C_0 is the geometry capacitance calculated as:

$$C_0 = \frac{\varepsilon_0 A}{d} = \frac{\varepsilon_0 \pi D^2}{4d} \quad (5)$$

2.3 TRANSMISSION/REFLECTION LINE TECHNIQUE

A measurement using the Transmission/Reflection line technique involves placing a sample in a section of the coaxial line and measuring the two ports complex scattering parameters with a vector network analyzer (VNA). The paper is wrapped around the inner conductor of the coaxial cable. The diagram of the test system is shown in Fig. 3. MUT stands for material under test.

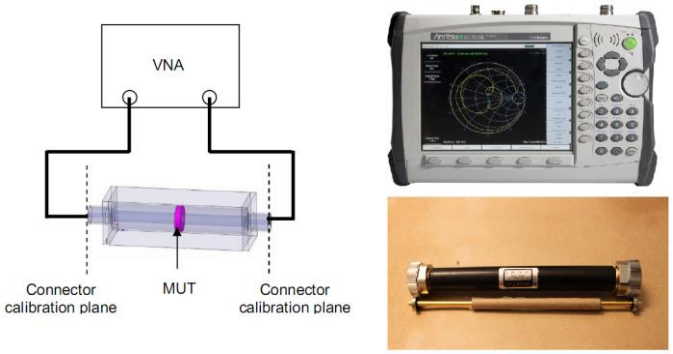

Fig. 3: The dielectric frequency response measurement system including VNA and coaxial line connected together

The relevant S-parameters relate closely to the permittivity of paper by the wave equations. The permittivity of the transformer paper can be obtained from the measured S-parameters. The term 'scattering' refers to the change of the traveling currents and voltages when they meet a discontinuity in the transmission line. S_{nm} represents the phase and magnitude of the electromagnetic wave sent by port m and received by port n.

The Kraft paper is partially filled in the coaxial line in this experiment for the ease of handling. However, full wave analysis is necessary to extract the permittivity information from the obtained scattering parameters due to the discontinuity.

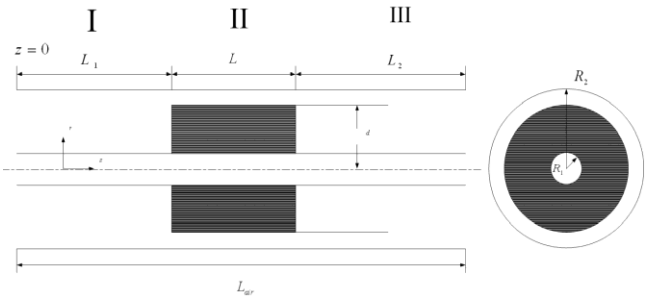

Fig. 4: Geometry of the partially filled coaxial line

Higher modes are excited due to the discontinuous structure shown in Fig. 4. The wave equation of the discontinuous structure needed to be solved is written as:

$$\left(\frac{\partial^2}{\partial r^2}+\frac{1}{r}\frac{\partial}{\partial r}+\frac{1}{r^2}\frac{\partial}{\partial \varphi^2}+k_c^2\right)E_z(r,\varphi)=0 \qquad (6)$$

where $k_c^2=\omega^2\varepsilon\mu+\gamma^2$, $E_z(r,\varphi)=e_z(r,\varphi)\cdot e^{-\gamma z}$.

Because of the azimuthal symmetry, $\partial/\partial\varphi=0$. The solution of the partial differential equation (6) is:

$$e_z(r,\varphi)=AJ_0(k_c r)+BY_0(k_c r)$$

And for this particular case, the solution is:

$$e_z(r,\varphi)=\begin{cases}AJ_0(k_d r)+BY_0(k_d r) & R_1<r<d\\ CJ_0(k_a r)+DY_0(k_a r) & d<r<R_2\end{cases} \qquad (7)$$

where $k_d^2=\omega^2\varepsilon_r\mu_0+\gamma^2$, $k_a^2=\omega^2\varepsilon_0\mu_0+\gamma^2$.

The magnetic field which is coupled with the electric field is given by:

$$H_\varphi=\frac{-j\omega\varepsilon}{k_c^2}\frac{\partial E_z}{\partial r} \qquad (8)$$

The propagation constants can be solved by the equations obtained from the boundary conditions. The boundary conditions are:

1) $e_z=0$ at $r=R_1$ and $r=R_2$

2) e_z and h_φ are continuous at $r=d$

The transverse electromagnetic field components in three sections (air-sample-air) can be written as:

$$E_{Ir}=\frac{A_0}{r}\left[e^{-\gamma_{I0}(z-L1)}+\Gamma_{I0}e^{\gamma_{I0}(z-L1)}\right]+\sum_{i=1}^{\infty}A_i Z_{I1}(k_{ci}r)\Gamma_{Ii}e^{\gamma_{Ii}(z-L1)} \qquad (9)$$

where A_0 is the amplitude of the incident electromagnetic wave in region I, Γ_{I0} is the magnitude of the reflected electromagnetic wave, the rest part is the expression for higher modes. In region I it assumes that there is only reflected higher modes wave due to fast attenuation of high modes. There is only forward TEM wave due to the matched impedance of the VNA. No TEM mode exists in Region II. Z_i has the same pattern as equation (7) with known propagation constants from boundary conditions. The rest five electromagnetic equations for three regions shown in Fig.4 are:

$$H_{I\varphi}=\sqrt{\frac{\varepsilon_0}{\mu_0}}\frac{A_0}{r}\left[e^{-\gamma_{I0}(z-L1)}-\Gamma_{I0}e^{\gamma_{I0}(z-L1)}\right]-\sum_{i=1}^{\infty}\frac{j\omega\varepsilon_0}{\gamma_{Ii}}A_i Z_{I1}(k_{ci}r)\Gamma_{Ii}e^{\gamma_{Ii}(z-L1)}$$

$$E_{IIr}=\sum_{m=1}^{\infty}B_m Z_{II1}\left(k_{cm}^{y}r\right)\cdot\left[e^{-\gamma_{II\,m}(z-L1-L)}+\Gamma_{II\,m}e^{\gamma_{I\,Im}(z-L1-L)}\right]$$

$$H_{II\varphi}=\sum_{m=1}^{\infty}\frac{j\omega\varepsilon^{y}}{\gamma_{II\,m}}B_m Z_{II1}\left(k_{cm}^{y}r\right)\cdot\left[e^{-\gamma_{II\,m}(z-L1-L)}-\Gamma_{II\,m}e^{\gamma_{I\,Im}(z-L1-L)}\right]$$

$$E_{IIIr}=\frac{C_0}{r}e^{-\gamma_{III0}(z-L_1-L-L_2)}+\sum_{n=1}^{\infty}C_n Z_{III1}(k_{cn}r)e^{\gamma_{IIIn}(z-L_1-L-L_2)}$$

$$H_{III\varphi}=\sqrt{\frac{\varepsilon_0}{\mu_0}}\frac{C_0}{r}e^{-\gamma_{III0}(z-L_1-L-L_2)}+\sum_{n=1}^{\infty}\frac{j\omega\varepsilon_0}{\gamma_{IIIn}}C_n Z_{III1}(k_{cn}r)e^{-\gamma_{IIIn}(z-L_1-L-L_2)}$$

Then, the orthogonality relation between different modes is applied at the boundaries $z=L_1$ and $z=L_1+L$:

$$\int_{R_1}^{R_2}E_{rm}H_{\varphi n}\cdot 2\pi r dr=0\left(z=L_1,\ z=L_1+L\right)\quad m\neq n$$

Set $A_0 = 1$ (the incident amplitude of the electromagnetic wave) and solve the system equations above to obtain A_1 and C_0. As the higher order modes decay very fast in the coaxial line, multiplying A_1 and C_0 with their phase factors according to the reference plane, S_{11} and S_{21} are obtained. In practice, S_{11} and S_{21} can be measured by VNA, then the inverse procedure reveals the permittivity of the Kraft paper.

3.0 SAMPLE PREPARATION

The Kraft paper is first heated in the vacuum oven at 140 °C for over 48 hours. The pressure inside the oven is kept below 1 mbar. After the drying process the moisture inside paper goes below 0.1% which is verified by the Karl Fischer titration [4]. Then it is impregnated with mineral oil and cool down to room temperature under vacuum.

Some salt solutions are then utilized to provide certain relative humidity in a closed chemical system (desiccators). Then the paper samples are kept in the desiccators for two weeks. The salts, their corresponding relative humidity and the moisture content of the conditioned samples are listed in Table 1.

Table 1. Relative humidity of the closed systems and sample moisture contents

Salt	Humidity (%)	Moisture (%)
Lithium bromide	1.8	<1
Lithium chloride	12.0	2.4
Potassium acetate	23.5	3.0
Sodium iodide	38.5	4.4
Sodium bromide	58	5.5

4.0 LOW FREQUENCY SPECTROSCOPY

Real and imaginary part of the complex permittivity below 1 MHz are shown in Fig. 5 and Fig. 6. There is considerable variation for both real and imaginary part of the complex permittivity below 100 Hz. As the frequency continuously increases, the differences between real part permittivity start to become smaller. The imaginary part of the complex permittivity with different moisture contents is quite low and seems to go to the same point at 1 MHz.

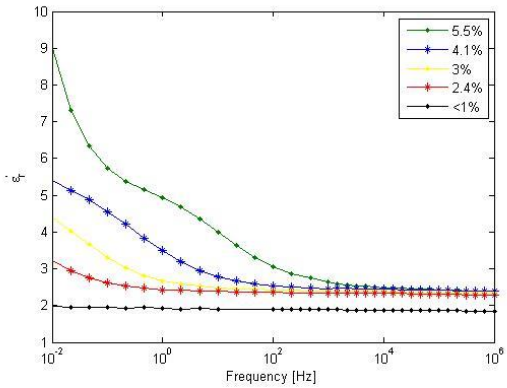

Fig.5: Low frequency real part of the complex permittivity with various moisture contents

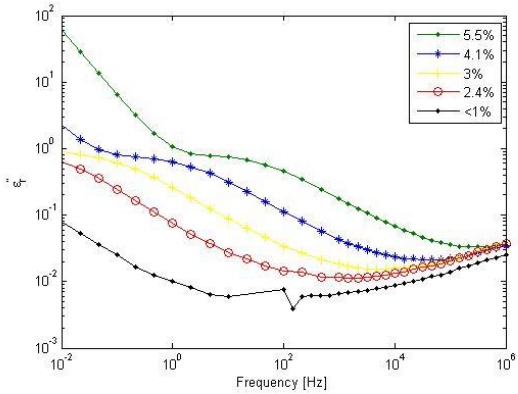

Fig.6: Low frequency imaginary part of the complex permittivity with various moisture contents

4.1 HIGH FREQUENCY SPECTROSCOPY

Figure 7 and Figure 8 show the high frequency real part and imaginary part of the complex permittivity respectively. The lower frequency limit is 100 MHz due to the limitation of the coaxial line. The most interesting phenomenon is that the imaginary part permittivity shifts to higher frequency with the increase of moisture content. The loss peak appears at 0.6 GHz when the moisture level is 5.5%. And the loss peak for 4.1% curve is around the beginning frequency i.e. 0.1 GHz. The shifted distance of these two curves is quite close to the low frequency spectroscopy at the logarithm scale. The loss peak for the other three curves cannot be observed due to the frequency blank between 1MHz to 100 MHz. At 3% moisture, loss decrease is slightly visible at the beginning frequency.

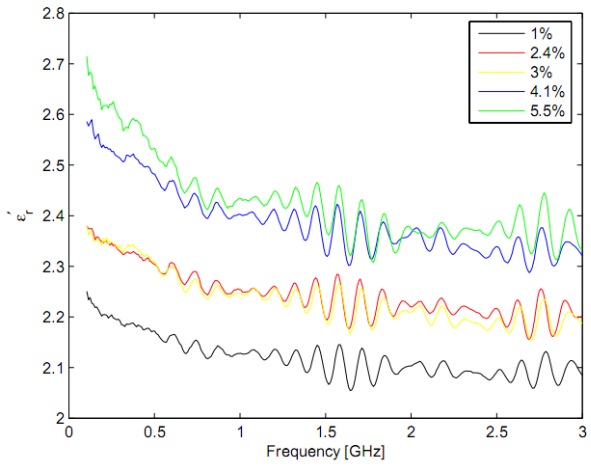

Fig.7: High frequency real part of the complex permittivity with various moisture contents

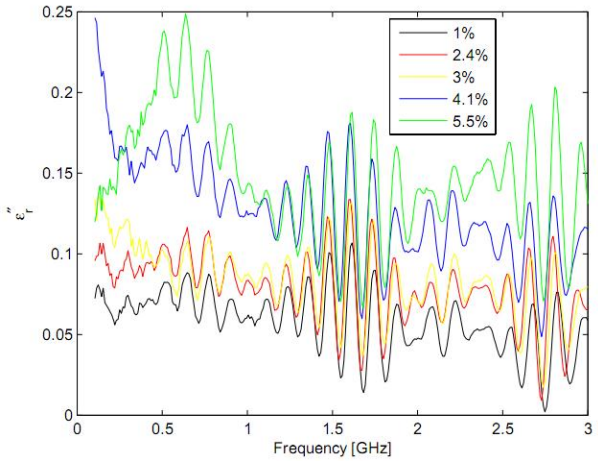

Fig.8: High frequency imaginary part of the complex permittivity with various moisture contents

5.0 DISCUSSION

The inner and outer diameters of the coaxial line utilized in the experiment are 3 mm and 7 mm respectively. These parameters make the coaxial line excellent for high frequency application. However, it sacrifices the accuracy of the lower frequency result. This is the reason that the starting frequency in high frequency range is 100 MHz instead of 1 MHz. On the other hand, the highest available output frequency of the VNA is 6 GHz. Better VNA with higher available frequency is needed because the loss peak of water is at 15 GHz [5]. Probably there will be another more significant loss peak at 15 GHz. The future work is to design a coaxial line with larger diameters so that the 1MHz to 100MHz spectroscopy blank could be covered. Better VNA is also preferred to cover the dispersion frequency of water.

6.0 CONCLUSION

This project was done mainly for the investigation of the moisture influence on Kraft paper insulation. The results so far prove that the moisture contributes to the increase of the conductivity, i.e. low frequency dispersion and the shift of loss peaks. Both real and imaginary part of the complex permittivity shows significant differences at frequencies below 100 Hz while the permittivity differences between 10 kHz and 1 MHz are not so remarkable. The loss peak frequency of the insulation material depends on the moisture content. The peak shifts to higher frequencies as the moisture increases.

Dielectric Frequency Response (DFR) technology is successfully applied on the diagnosis of power transformers in field for decades. It is an off-line method which has been widely used and well proven. The frequency range of the available units on the market so far is from 0.1 mHz to 10 kHz. This range is the most efficient and effective for the transformer insulation diagnostics so far. The high frequency property of the insulation material will be valuable in future for the on-line transformer diagnostic techniques with the help of antennas.

7.0 REFERENCES

[1] U. Gafvert; L. Adeen, M. Tapper, P. Ghasemi, P. and B. Jonsson, “Dielectric spectroscopy in time and frequency domain applied to diagnostics of power transformers,” Proceedings of the 6th International Conference on Properties and Applications of Dielectric Materials, 825-830, 2000.

[2] L.E. Lundgaard, D. Linhjell, O.L. Hestad, and J.-T. Borlaug, “High frequency dielectric response of paper/oil insulation,” IEEE International Conference on Dielectric Liquids, 2008. ICDL 2008.

[3] W. C. Heerens and F. C. Vermeulen, “Capacitance of Kelvin guard-ring capacitors with modified edge geometry,” Journal of Applied Physics, vol. 46, no. 6, p. 2486, 1975.

[4] Peter A. Bruttel, Regina Schlink, “Water determination by Karl Fischer Titration,” Metrohm AG.

[5] U. Kaatze, “Complex permittivity of water as a function of frequency and temperature,” Journal of Chemical & Engineering Data, vol. 34, pp. 371–374, Oct. 1989.